



## Deoxygenation of the Gulf of Mexico thermocline linked to a decrease in the detachment frequency of Loop Current Eddies

José Quintanilla<sup>1</sup>, Juan Carlos Herguera<sup>2</sup>, Julio Sheinbaum<sup>1</sup>

<sup>1</sup> Departamento de Oceanografía Física, Centro de Investigación Científica y de Educación Superior de, Ensenada, Mexico.

<sup>2</sup> Departamento de Ecología Marina, Centro de Investigación Científica y de Educación Superior de, Ensenada, Mexico.

Correspondence to: José G. Quintanilla ([jquintan@cicese.edu.mx](mailto:jquintan@cicese.edu.mx))

**Abstract.** This study presents an oxygen time series of the Gulf Mexico deep water region spanning from 2010 to 2019 using data from 6 oceanographic cruises and one ARGO buoy. The data suggest a deoxygenation trend in the thermocline of the Gulf of Mexico. This deoxygenation trend seems to be connected to a reduction in the number of eddies that detached from the Loop Current from 2010 to 2019 observed with altimetry data from the last two decades, and although the average size of the mesoscale structures shows a slight increase, the average detached area per year almost halved from the 2000–2010 decade to the 2010–2020 decade. Using the oxygen measurements and the altimetry data, a simple box model was formulated to reproduce the measured oxygen temporal variability in the GoM main thermocline from 2000 to 2020. The results from the box model suggest that an average detached Loop Current Eddy area of about 90 000 km<sup>2</sup> per year is needed in order to maintain constant oxygen levels in the main thermocline waters. This threshold wasn't reached during the 2010 to 2020 decade and if the LCE detachment area per year continues to decrease in the future, oxygen concentrations in the Gulf of Mexico thermocline might continue to fall with still unknown effects in the ecological web structure at these depths.

### 1 Introduction

Deoxygenation of a volume of water occurs when the rate of oxygen consumption becomes higher than the rate of oxygen supply, in the ocean both of those rates are controlled by various mechanisms that are particular to the oceanic region and depth (Pitcher et al., 2021). Such decrease of the oxygen concentrations ([O<sub>2</sub>]) in coastal and open ocean waters is an alarming global trend associated with anthropogenic forcing and climate change (Oschlies et al., 2018). In the open ocean in particular, intermediate and deep-water deoxygenation has been linked to a decrease of the oxygen content in subducting water masses, driven mainly by ocean warming, as well as to an increased stratification that reduces the fluxes of currents that ventilate those depths (Falkowski et al., 2011; Portela et al., 2020).

Among the processes that ventilate the thermocline waters of the open ocean, the role of mesoscale eddies has been observed but not extensively reported because of the limitation of observational methods and the highly variable nature of mesoscale circulation (Gruber et al., 2010; Levin, 2018). The GoM is an oceanic region where the effect of mesoscale eddies in the



35 oxygen content of its volume can be easier to observe than in other bigger basins, because it is a semi enclosed sea heavily  
influenced by the mesoscale circulation that transports Caribbean water in to its interior (Meunier et al., 2018).

While the principal deoxygenation concern in the GoM is the expanding low oxygen “dead zone” of the northern shelf waters  
(Rabalais et al., 2002), in the Gulf’s deep-water region (here delimited as the region with depths greater than 1000 m, Figs.  
40 1a, 2a and 3) measurements obtained during the last decade suggest a deoxygenation trend in the main thermocline (Table  
1), that has not been previously addressed. For the purposes of this paper the main thermocline of the GoM is defined as the  
volume of water with a potential density anomaly between 26.3 and 27.25 kg m<sup>-3</sup> (highlighted with the shadowed red and  
blue ranges in Figs. 1c and 2b) within the 200–800 m depth range. Relatively low oxygen values ([O<sub>2</sub>] < 2.8 ml l<sup>-1</sup> (< 120  
μmol kg<sup>-1</sup>) were historically only measured in the lower boundary of the main thermocline west of 90° w, but recent  
45 observations indicate these relatively low concentrations extend to the entire main thermocline (Table 1, Figs. 1b, 2b and 3).  
It’s important to study the possible causes of this effect as a continued deoxygenation of this volume of water could impact  
the mobile macroorganisms populations with high economic and ecological value that are either stressed or migrate away in  
low oxygen conditions (Stramma et al., 2010; Andrews et al., 2017).

50 The highest [O<sub>2</sub>] in the GoM main thermocline have historically been measured in the eastern region (Table 1, Figs. 1c and  
2b), where the highly energetic Yucatan Current transports Caribbean water through the Yucatan Channel into the Gulf and  
becomes the Loop Current (LC) that either extends and intrudes into the northeastern GoM before exiting through the Florida  
Straits to the Atlantic or goes port to port with no intrusion (Maul, 1977; Hurlburt and Thompson, 1980; Athié et al., 2020).  
The oxygen content of the main thermocline in the Caribbean is higher than in the GoM, as it shows a decreasing gradient  
55 from northeast to southwest, where GoM common waters with higher residence time are usually located (Rivas et al., 2005).

The main thermocline of the LC is delimited by two water masses that are clearly identifiable by their contrasting oxygen  
content (Morrison and Nowlin, 1977). In its upper boundary, at a potential density anomaly range of  $\sigma_{\theta}$ : 26.3 to 26.6 kg m<sup>-3</sup>,  
the Eighteen degree water (EDW, also often referred as the 18° Sargasso Sea Water and the North Subtropical Mode Water)  
60 is usually identified by a local [O<sub>2</sub>] maximum (Figs. 1c and 2b). The relatively high [O<sub>2</sub>] of this water mass is the result of a  
nearly uniform temperature over a deep mixed layer during winter in the northern Sargasso Sea where it originates (Kwon  
and Riser, 2004; Billheimer et al., 2021). In the Caribbean, it was first reported in the eastern Venezuelan Basin with an [O<sub>2</sub>]  
of 3.8 ± 0.2 ml l<sup>-1</sup> (Kinard et al., 1974) and in the LC in the eastern GoM with oxygen values of 3.6 ± 0.2 ml l<sup>-1</sup>, (Morrison  
and Nowlin, 1977). The lower boundary of the LC main thermocline, centered at  $\sigma_{\theta}$ : 27 to 27.25 kg m<sup>-3</sup>, is filled with the  
65 Tropical Atlantic central water (TACW), identified in the LC with an [O<sub>2</sub>] minimum of 3.05 ± 0.2 ml l<sup>-1</sup> (Morrison and  
Nowlin, 1977). (In this work the usual convention of mean ± one standard deviation is used to report values).



In comparison with the oxygen levels measured in the thermocline of the LC, the thermocline of the western GoM has lower [O<sub>2</sub>] (Table 1, Fig. 1 and 2), implying a longer residence time inside the GoM (Rivas et al., 2005). The highest contrast is observed in the upper thermocline at  $\sigma_\theta = 26.5 \text{ kg m}^{-3}$ , where a gradual oxygen decrease from east to southwest of up to  $0.8 \text{ ml l}^{-1}$  erodes the local oxygen maximum that identifies the EDW in the Caribbean and in the LC (Jochens et al., 2005). The lower thermocline shows a similar though lower decrease in [O<sub>2</sub>] values of  $0.35 \text{ ml l}^{-1}$  with respect to the LC (Morrison et al., 1983). The clear contrast between the oxygen content of the LC and the western GoM makes it a non-conservative property that can be used to evaluate the water exchange between the LC and the GoM interior.

Assuming that the ventilation of the GoM main thermocline is controlled by the exchange of water between the relatively highly oxygenated LC and the GoM (Rivas et al., 2005), the observed contrasting oxygen values between the LC and the central and western GoM imply a relatively low exchange between the LC and the Gulf interior waters. Indeed, the annual volume exchanged for in upper 700 m between both regions has been estimated to be of only 10% of the annual LC flow and most of this exchange was estimated to occur during the sporadic events of Loop Current Eddies (LCE) detachments (Maul, 1980). The detachment frequency of these mesoscale structures is highly variable, occurring every 2 to 18 months (Leben, 2005), their size is also highly variable with diameters ranging from 200 to 400 km (Elliot, 1982) and their depth of influence has been estimated to be of up to 1000 m (Meunier et al., 2018). Once detached, these eddies transport water with the characteristics of the LC into the GoM basin (Meunier et al., 2020), slowly mixing the transported volume with the Gulf's interior water until it loses all coherence usually at the western GoM (Meunier et al., 2018). Hence, changes in the exchanged volume between the LC and the western GoM driven by the variability of the detached LCE volume could lead to changes in the oxygen content of the main thermocline of the GoM interior waters.

Although the difference between the oxygen concentrations of the eastern and the western GoM has been widely reported, the oxygen of the main thermocline of the deep GoM was considered to stay relatively constant with time (Jochens et al., 2005). In the deep GoM, the only ARGO float equipped with oxygen sensors (Biogeochemical ARGO, buoy) was deployed in June 2010, increasing the available oxygen measurements in its main thermocline waters (Fig 1 and 2). The deployment was made in the eastern GoM inside the LCE Franklin and from there it drifted alongside the LCE until April of 2013 (Fig. 2). The measurements showed that [O<sub>2</sub>] for the upper and lower thermocline are lower than previously measured in the eastern GoM with values of  $3.25 \text{ ml l}^{-1}$  and  $2.54 \text{ ml l}^{-1}$  respectively (Table 1). This trend towards lower values was further observed in the western GoM with oxygen sensors on gliders measuring values below  $2.74 \text{ ml l}^{-1}$  and  $2.4 \text{ ml l}^{-1}$  in the upper and lower thermocline respectively (Portela et al., 2018).

In the North Atlantic it has been suggested that oxygen transport by the eddies could be an important mechanism for the ventilation of the thermocline waters (Robbins et al., 2000; Brandt et al., 2015; Hanh et al., 2017; Pitcher et al., 2021). The semi-enclosed character of the GoM basin allowed to study the implications of this process on the ventilation of the main



thermocline with less intrusion from other physical mechanisms than in larger basins. The identification of LCE detachments has been commonly used to understand the circulation in the GoM (Leben, 2005; Hall and Leben, 2016), and this study follows the previously reported methodology to compute the date of LCE detachments and their approximate area from 2000 to 2019 using AVISO SSH data. Using the LCE calculated metrics, a simple box model parametrized with the oxygen measurements was formulated in order to reproduce the variability in the main thermocline.

**Table 1**

Previously reported and here presented mean oxygen concentrations in the upper and lower thermocline of the Gulf of Mexico east of 90° and west of 90°

<b>Mean [O<sub>2</sub>] in the upper and lower main thermocline of the deep Gulf of Mexico (ml l<sup>-1</sup>, μmol kg<sup>-1</sup>)</b>			
<b>East of 90° W (Loop Current and Yucatan Channel *Caribbean not included)</b>		<b>West of 90° W (Central and Western Gulf of Mexico)</b>	
$\sigma_{\theta}$ (kg m <sup>-3</sup> )	$\sigma_{\theta}$	$\sigma_{\theta}$	$\sigma_{\theta}$
26.3-26.6	27-27.15	26.3-26.6	27-27.25
<b>3.6 ± 0.20</b>	<b>3.05 ± 0.20</b>	<b>3.0 ± 0.20 *</b>	<b>2.7 ± 0.20</b>
156.6 ± 8.7	132.6 ± 8.7	130.5 ± 8.7	117.4 ± 8.7
1972	1972	1978	1978
Morrison and Nowlin, 1977	Morrison and Nowlin, 1977	Morrison et al., 1983	Morrison et al., 1983
<b>3.4 ± 0.20 *</b>	<b>2.8 ± 0.20 *</b>		
147.9 ± 8.7	121.7 ± 8.7		
1999 - 2000	1999 - 2000		
Rivas et al., 2005	Rivas et al., 2005		
<b>3.3 ± 0.30 *</b>	<b>2.8 ± 0.20 *</b>	<b>3.0 ± 0.20 *</b>	<b>2.7 ± 0.15 *</b>
143.6 ± 13.1	121.7 ± 8.7	130.5 ± 8.7	117.4 ± 6.2
2000 - 2001	2000 - 2001	2000 - 2001	2000 - 2001
Jochens and DiMarco, 2008	Jochens and DiMarco, 2008	Jochens and DiMarco, 2008	Jochens and DiMarco, 2008
<b>3.23 ± 0.25</b>	<b>2.54 ± 0.07</b>	<b>2.75 ± 0.25 **</b>	<b>2.40 ± 0.20 **</b>
140.5 ± 10.9	110.4 ± 3	119.6 ± 10.9	104.4 ± 8.7
2010 - 2013	2010 - 2013	2010 - 2017	2010 - 2017
BioARGO Buoy	BioARGO Buoy	Portela et al., 2018	Portela et al., 2018
<b>3.37 ± 0.21</b>	<b>2.66 ± 0.08</b>	<b>2.75 ± 0.17</b>	<b>2.46 ± 0.07</b>
147.1 ± 8.1	116.26 ± 3.6	119.7 ± 7.2	107.1 ± 3.2
2011 - 2019	2011 - 2019	2011 - 2019	2011 - 2019
XIXIMI cruises	XIXIMI cruises	XIXIMI cruises	XIXIMI cruises

\* Estimates based on figures

\*\* Data from anticyclonic eddies





## 2 Methods

### 2.1 Oxygen data

The oxygen data used for this study came from the XIXIMI cruises, carried out by the Consorcio de Investigación del Golfo de México (CIGoM) aboard the RV/Justo Sierra from 2011 to 2019 in the dates listed on Table 2. Oxygen values from the XIXIMI cruises were measured with a CTD equipped with a calibrated SBE43 oxygen sensor and the data was calibrated on board following the microwinkler method (Furuya and Harada, 1995). The array of stations was intended to be as similar as possible between cruises, with a spatial resolution of approximately 1° (Figs. 1 and 3). In the sampling during the XIXIMI-5 cruise the center of LCE Poseidon was sampled, and during the XIXIMI-6 and 7 cruises samples from the upper north Caribbean basin were taken, as well as during XIXIMI-7 when four extra stations were sampled in the northwestern GoM. Unfortunately, the “Nortes” (northern winds) during XIXIMI-3 and tropical cyclones during XIXIMI-6 and 7 did not allow the sampling of all planned stations during these cruises (Fig. 3). In spite of these gaps, the sampled area is considered representative of the deep GoM region as it encompasses a considerable area over time, including stations in the Yucatan Channel and in the northwestern Caribbean (Figs. 1 and 2).

125

In addition, oxygen measurements from the Biogeochemical ARGO float *aoml 4901043* (<http://ARGO.jcommops.org>) were used to provide value comparisons with the XIXIMI cruises as well as to get spatial coverage of the north eastern deep GoM. The BioARGO measurements presented here (Table 1, Figs. 1 and 2) are the raw measurements without any post-calibration work, as such, the sensor might present offset and drift errors of up to 5% per year after its deployment (Bushinsky et al., 2016). A correction technique in the absence of near calibrated oxygen measurements has been suggested that employs WOCE climatology to correct first order errors (Takeshita et al., 2013). Following this method, however, would bias the float data towards a climatology based on 1980–90’s data, hiding to some extent any deoxygenation trend of the last decade. Even accounting for sensor errors, the BioARGO measurements show a decrease of oxygen from previously measured concentrations (Table 1) above the precision or drift errors reported for the sensor (Uchida et al., 2008).

135

The TEOS-10 algorithms (McDougall and Barker, 2011) were used to calculate absolute salinity, potential temperature and potential density (both referenced to the surface) from de CTD measurements. The upper and lower thermocline were identified as the density range from 26.3 to 26.6 kg m<sup>-3</sup> and 27 to 27.25 kg m<sup>-3</sup> respectively, following similar ranges previously reported (Table 1) and ensuring that both the [O<sub>2</sub>] local maximum of the EDW in the LC and the [O<sub>2</sub>] minimum of the TACW in the LC and the western GoM were fully encompassed (the mid thermocline waters presents transitional [O<sub>2</sub>] values between these two extremes, and we chose not to focus them here).

140



[O<sub>2</sub>] values are reported in the text and figures in ml l<sup>-1</sup> to be consistent with the historically reported units in GoM studies (Table 1). However, as the units μmol kg<sup>-1</sup> are most commonly reported in the recent literature, we made the conversion to these units using the TEOS–10 equation based on the calculated potential density.

145

The mean [O<sub>2</sub>] values in the upper and lower main thermocline were calculated for every profile of the XIXIMI cruises and the BioARGO float. With the objective of simplifying the visualization of the data and the comparison between cruises, each entire profile was labeled with a color code according, only, to the mean oxygen value in the upper main thermocline in the density range from 26.3 to 26.6 kg m<sup>-3</sup> (where the [O<sub>2</sub>] spatial and temporal change were more pronounced) using the following criteria (in parenthesis the color code applied in Figs. 1, 2 and 3).

150

- Loop Current Water (red): [O<sub>2</sub>] > 3.25 ml l<sup>-1</sup> (142 μmol kg<sup>-1</sup>)
- Transition Water 1 (orange): 3–3.25 ml l<sup>-1</sup> (131–142 μmol kg<sup>-1</sup>)
- Transition Water 2 (cyan): 2.75–3 ml l<sup>-1</sup> (120–131 μmol kg<sup>-1</sup>)
- Resident Water of the GoM interior (blue): [O<sub>2</sub>] < 2.75 ml l<sup>-1</sup> (120 μmol kg<sup>-1</sup>)

155

The map of locations of the XIXIMI stations and BioARGO profiles (Fig. 1a) as well as the [O<sub>2</sub>] profiles plotted against depth (Fig. 1b) and against potential density anomaly (Fig. 1c) are presented with the aforementioned color coding. The mean depths for the upper and lower thermocline of the LC were estimated using all the profiles identified as Loop Current water while the mean depths for the upper and lower thermocline of the GoM were estimated using all the profiles identified as transition water 1 and 2 and resident water (shown in Fig. 1b).

160

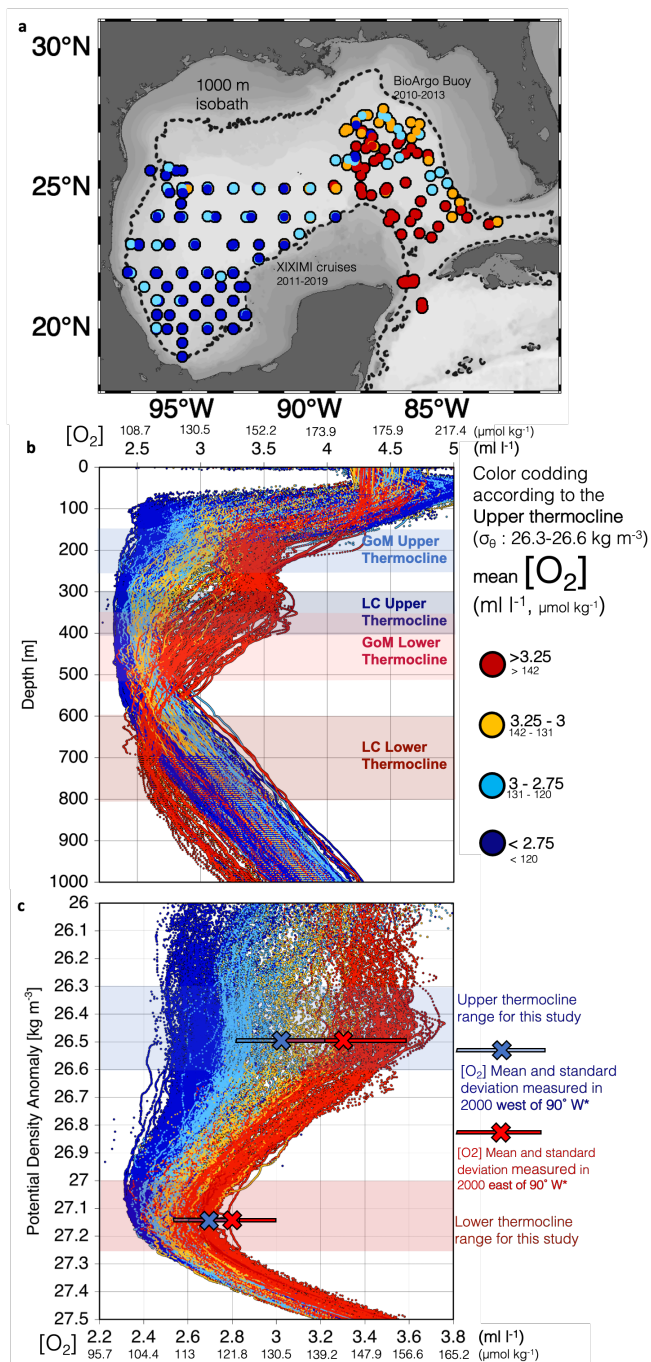


**Figure 1: (a) Map of BioARGO profiles and XIXIMI sampled stations during 6 oceanographic campaigns from 2010 to 2019, (b) Depth vs [O<sub>2</sub>] profile for all stations, (c) Close up to the isopycnal range of the main thermocline of the potential density vs [O<sub>2</sub>] profile for all stations. \*Jochens and DiMarco, 2008.**



**Table 2**

Date of campaigns and mean Oxygen concentrations in the upper and lower thermocline for the Loop Current and Gulf interior water

Campaign	Date	Mean thermocline O <sub>2</sub> (ml l <sup>-1</sup> , μmol kg <sup>-1</sup> )					
		Loop Current Water		n (Number of profiles)	Gulf Interior Water		n
		Upper 26.3-26.6	Lower 27-27.25		Upper 26.3-26.6	Lower 27-27.25	
Bio ARGO	13/06/2010 to 14/04/2013	<b>3.39 ± 0.12</b> 147.72 ± 5.72	<b>2.57 ± 0.06</b> 115.94 ± 2.89	32	<b>2.98 ± 0.17</b> 123.47 ± 6.73	<b>2.52 ± 0.06</b> 110.00 ± 3.42	44
XIXIMI-2	2/07/2011 to 12/07/2011	<b>3.55 ± 0.08</b> 152.23 ± 5.2	<b>2.74 ± 0.05</b> 118.39 ± 3.49	7	<b>2.78 ± 0.17</b> 120.92 ± 5.47	<b>2.50 ± 0.04</b> 108.47 ± 2.06	33
XIXIMI-3	13/02/2013 to 10/03/2013	<b>3.56 ± 0.06</b> 154.07 ± 2.57	<b>2.68 ± 0.05</b> 117.24 ± 2.33	3	<b>2.82 ± 0.12</b> 122.54 ± 4.93	<b>2.52 ± 0.07</b> 109.77 ± 3.54	33
XIXIMI-4	27/08/2015 to 16/09/2015	<b>3.45 ± 0.06</b> 150.67 ± 3.02	<b>2.74 ± 0.04</b> 119.12 ± 2.35	11	<b>2.88 ± 0.22</b> 125.39 ± 8.17	<b>2.49 ± 0.09</b> 108.49 ± 4.42	44
XIXIMI-5	10/06/2016 to 24/06/2016	<b>3.28 ± 0.07</b> 142.76 ± 3.14	<b>2.66 ± 0.05</b> 116.46 ± 2.79	5	<b>2.84 ± 0.11</b> 123.35 ± 4.77	<b>2.50 ± 0.06</b> 108.51 ± 2.91	35
XIXIMI-6	19/08/2017 to 7/09/2017	<b>3.49 ± 0.07</b> 151.76 ± 2.91	<b>2.69 ± 0.06</b> 117.33 ± 2.73	12	<b>2.65 ± 0.05</b> 115.51 ± 2.76	<b>2.41 ± 0.05</b> 104.79 ± 2.45	36
XIXIMI-7	9/05/2019 to 7/06/2019	<b>3.31 ± 0.07</b> 149.16 ± 2.95	<b>2.68 ± 0.04</b> 117.11 ± 2.03	10	<b>2.61 ± 0.09</b> 113.76 ± 4.13	<b>2.40 ± 0.05</b> 104.29 ± 2.09	22
<b>Mean O<sub>2</sub></b>		<b>3.49 ± 0.12</b> 150.96 ± 4.87	<b>2.66 ± 0.08</b> 117.85 ± 2.67	<b>80</b>	<b>2.78 ± 0.18</b> 121.03 ± 8.27	<b>2.47 ± 0.09</b> 107.39 ± 3.78	<b>247</b>

165

## 2.2 Loop Current and Loop Current Eddies data

The LC and LCE metrics were computed from the Global Ocean gridded L4 sea surface heights and derived variables reprocessed 1993 ongoing product distributed by Copernicus (<https://doi.org/10.48670/moi-00148>). In accordance with Leben (2005) and Hall and Leben (2016), the daily gridded SSH dataset from 1 January 2000 to 31 December 2019 was used to identify the LC and LCEs position tracking the 17 cm SSH contour. The LCT program identifies the time the 17 cm contour from the LC breaks. For this work the detachment date of a LCE was estimated as the initial date that the LC 17 cm contour

170



separated in two portions without any subsequent reattachment. The area of the LCE was computed as the average area and standard deviation of the daily area of the 17 cm contour during the first 30 days after the day of the identified detachment. 175 This 30-day period was arbitrary selected as a period representative of the LCE area after its detachment, the standard deviation of the identified LCEs area was in average close to  $\pm 10\%$ . The detachment date and LCE area (Fig. 4) were used to compare the LCE detachment frequency and the total detached area during the 2000–2009 and 2010–2019 decades and were used also as parameters in the box model described in section 4. The computed LC and LCE positions are represented in Fig. 3 as surface maps that depict the mean SSH 17 cm contour during the days that the cruise took place, together with 180 monthly average values of the SSH 17 cm contour at 3, 6, 9, and 12 months prior to the date the cruises took place.

### 3 Results and discussions

#### 3.1 A decreasing trend in the oxygen content of the main thermocline

185 All the oxygen data used for this work is grouped in Fig. 1. In Fig. 1a the station map shows the location of all the XIXIMI and BioARGO profiles with the color coding according to the upper thermocline oxygen values in order to show the  $[O_2]$  spatial variability. Figure 1b shows the  $[O_2]$  profiles plotted against depth from 0 to 1000 m, the mean depth of the upper and lower thermocline ranges is shown as a shadowed interval in order to show the depth difference of the isopycnals in the LC and in the GoM interior. Figure 1c shows the  $[O_2]$  profiles plotted against the potential density anomaly from 26 to 27.5 kg  $m^{-3}$ , as a zoom in the thermocline density range. Plotting the oxygen against density makes it easier to compare the oxygen 190 values of the thermocline in the LC and in the GoM as it removes the isopycnal depth difference caused by the Loop Current and the mesoscale circulation.

Figure 1a shows the aforementioned gradual oxygen decrease from the Caribbean and eastern GoM to the southwestern GoM, 195 with maximum upper thermocline concentrations ( $[O_2]^{UT}$ ) above 3.25  $ml\ l^{-1}$  in what can be considered as the area filled with Caribbean and LC waters (Figure 1a). In agreement with this pattern, in every XIXIMI cruise and BioARGO profile, the highest mean values of  $[O_2]^{UT} \geq 3.25\ ml\ l^{-1}$  and  $[O_2]^{LT} \geq 2.6\ ml\ l^{-1}$  corresponding to upper and lower thermocline waters respectively, were only observed in the Caribbean, the Yucatan Channel and inside the GoM at a maximum LC western penetration of 87° W.

200 The BioARGO oxygen profiles were mainly taken inside the LC area of influence east of 90° W (Fig. 2). 32 of the total 76 BioARGO profiles had a mean upper thermocline  $[O_2]^{UT}$  equal or above 3.25  $ml\ l^{-1}$ , considered as LC water, 24 profiles were considered as transition waters 1, 16 as transition waters 2, and only 4 profiles presented mean values below 2.75  $ml\ l^{-1}$  and were considered as resident water of the GoM interior. The XIXIMI data shows a similar pattern with the highest  $[O_2]^{UT}$  205 values located in the LC area.

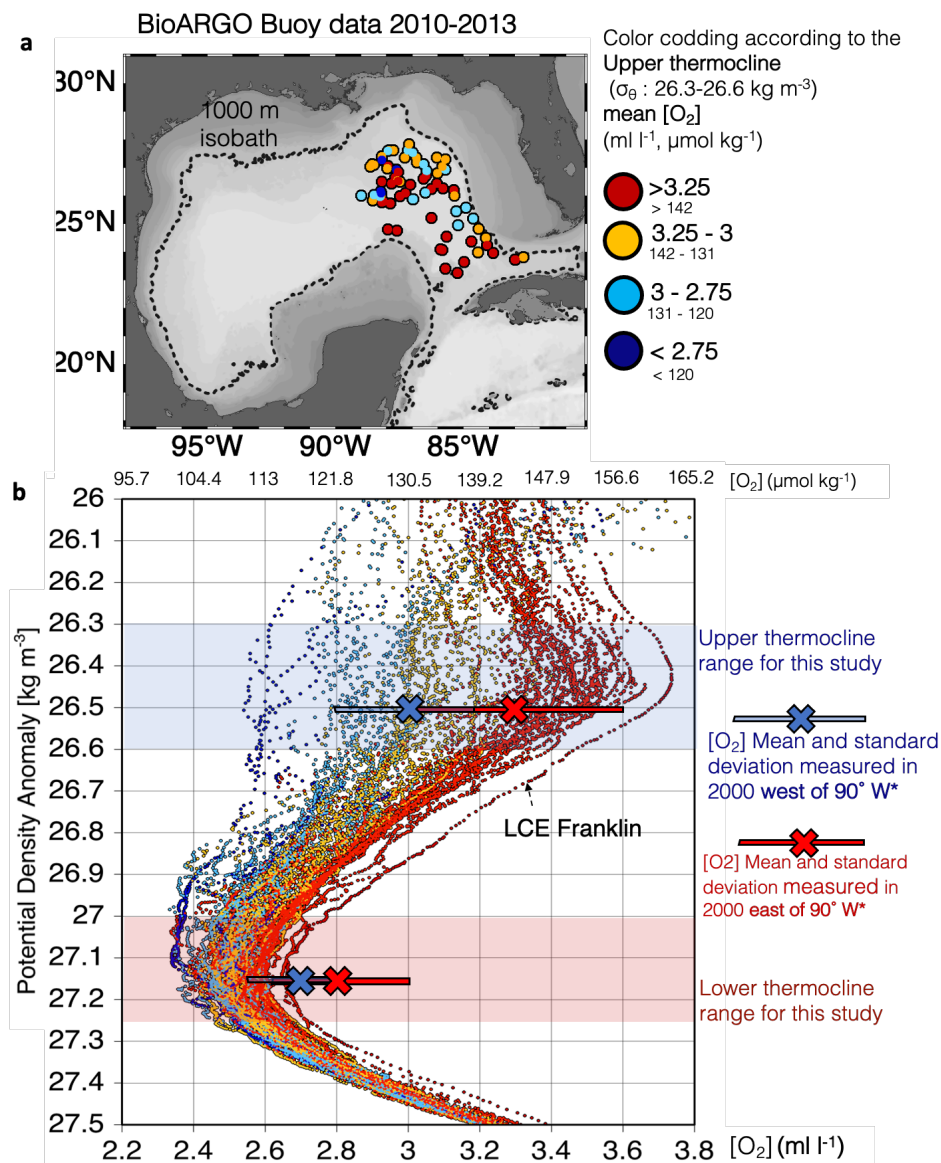


**Figure 2: (a) Map of BioARGO profiles from 2010 to 2013, (b) Close up to the isopycnic range of the main thermocline of the potential density vs [O<sub>2</sub>] profile for all stations. \*Jochens and DiMarco, 2008.**

210 A comparison between the previously reported oxygen measurements and the 2010-2019 XIXIMI and BioARGO data (Table 1, Figs. 1 and 2) highlights the following observations:

- East of 90° W the oxygen concentrations in the upper thermocline seem to have remained in the same levels in the last two decades, ranging from a minimum mean of  $[O_2]^{UT} = 3.23 \pm 0.25$  ml l<sup>-1</sup> measured by the BioARGO buoy to a maximum mean of  $3.40 \pm 0.20$  ml l<sup>-1</sup> measured in 2000 (Rivas et al., 2005), with the 2011 to 2019 XIXIMI mean falling in between at  $3.37 \pm$



215 0.21 ml l<sup>-1</sup>. This observation suggests that any change in the oxygen content of the upper thermocline of the GoM interior cannot be attributed to changes in the LC source waters.

- East of 90° W the oxygen concentrations in the lower thermocline seem to have decreased in the last two decades from a mean  $[O_2]^{LT} = 2.8 \pm 0.25$  ml l<sup>-1</sup> measured in 2000 (Rivas et al., 2005, Jochens and DiMarco, 2008) to a mean  $2.66 \pm 0.08$  ml l<sup>-1</sup> measured during the XIXIMI cruises and  $2.54 \pm 0.07$  ml l<sup>-1</sup> measured by the BioARGO buoy. Recent measurements have  
220 identified the TACW in the Eastern Caribbean with an oxygen minimum that is below 2.8 ml l<sup>-1</sup> (<120 μmol kg<sup>-1</sup>) (Van Der Boog et al., 2019), in the western Caribbean (Carrillo et al., 2016) and in the LC (Portella et al., 2018). This suggests the existence of a deoxygenation trend in the lower thermocline of the Caribbean that is happening outside the GoM that could be in part responsible for a deoxygenation trend of this isopycnic range inside the GoM.

- West of 90° W the oxygen concentrations in the main thermocline have decreased from mean values of  $[O_2]^{UT} = 3.0 \pm 0.20$   
225 ml l<sup>-1</sup> and  $[O_2]^{LT} = 2.7 \pm 0.20$  ml l<sup>-1</sup> in 1978 and in 2000 (Morison et al., 1983 and Jochens and DiMarco, 2008) to mean concentrations of  $2.75 \pm 0.20$  ml l<sup>-1</sup> and  $2.46 \pm 0.07$  ml l<sup>-1</sup> in the upper and lower thermocline respectively measured in average during all the XIXIMI cruises, similar values were also reported with glider measurements from 2010 to 2017 (Portela et al., 2018).

230 These observations suggest that during the last two decades any changes in the oxygen content of the upper thermocline of the deep GoM can be attributed to processes within the basin proper and not due to changes in the LC source waters, while any change in the oxygen content of the upper thermocline of the deep GoM can be attributed to changes in the LC source water and maybe also to changes attributed to processes within the basin proper. The time series obtained by the XIXIMI cruises can be useful to get more clarity about the process that could be responsible for a deoxygenation trend.

235

In order to observe the oxygen temporal and spatial variability during the 2010-2020 decade, Fig. 3 shows the individual  $[O_2]$  measurements from each of the six XIXIMI cruises from 2011 to 2019 in the deep GoM, using the same color scheme described in the methods. The surface maps also include the mean SSH 17 cm contour of the LC and LCEs tracked during the campaign period and the mean SSH 17 cm contour location 3, 6, 9, and 12 months prior to the surveys. Fig. 3 is described  
240 in detail in the following section.



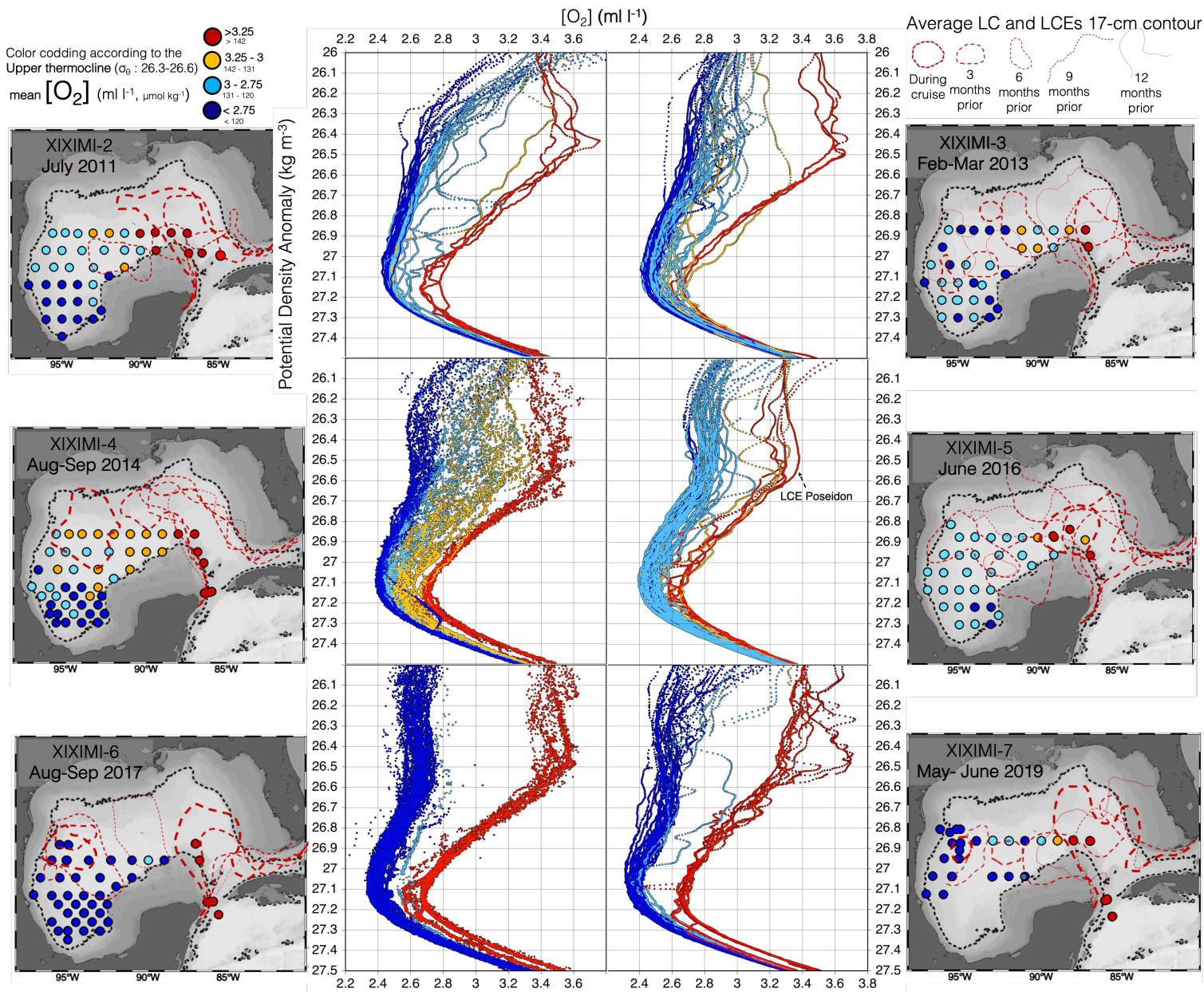


**Figure 3.** Oxygen profiles with density for the six XIXIMI cruises with color scheme following the described methodology. Maps of stations in each cruise follow the same color scheme. The 17 cm contour altimetry during the month of the expeditions and 3, 6, 9 and 12 months prior, is shown in the maps as the red discontinued lines that get more degraded the further from the cruise date.

245

During the XIXIMI-2 cruise (July 2011) the distribution of stations according to their upper thermocline oxygen concentration ( $[O_2]^{UT}$ ) was as expected; LC stations in the eastern Gulf, followed by transition stations in the central Gulf,



showing a mean  $[O_2]^{UT}$  between 2.75 and 3 ml l<sup>-1</sup>, and the lowest concentrations were consistently found in the southwestern region and the Campeche Bay. During this expedition the 17 cm SSH contour was localized in the eastern region of the LC, the last big LCE detachment (Franklin, area:  $a_{LCE} = 52\,133 \pm 2700$  km<sup>2</sup>) occurred 12 months before the expedition.

The following cruise took place in February and March 2013, this is the only XIXIMI cruise that took place during the winter season and the observations indicate no evident changes in the vertical structure of the permanent thermocline. During the expedition strong cold front winds (“Nortes”) didn’t allow the completion of the 24° N line. In comparison with the previous expedition, in XIXIMI-3 the green transition stations and the blue resident waters seemed to have been more mixed, without a clear north south distribution. In the 25° N line there were four stations with  $[O_2]^{UT} \leq 2.75$  ml l<sup>-1</sup> and three stations in the Campeche Bay with  $[O_2]^{UT} \geq 2.75$  ml l<sup>-1</sup>. Although during the expedition the LC was relatively retracted to the east, the 17 cm SSH contour of the huge LCE Jumbo ( $a_{LCE} = 92078 \pm 4500$  km<sup>2</sup>) that detached nine months before was still observed in the western GoM. The evolution of this eddy from the LC region to the western GoM shelf can be seen in the SSH 17 cm contours 3, 6, and 9 months prior to the cruise, and could explain the presence of relatively high thermocline  $[O_2]$  observed in the south west GoM. This suggests that the eddy still carries some volume of water with higher oxygen concentrations than its surrounding waters even nine months after its detachment from the LC.

The XIXIMI-4 cruise in August and September of 2015 was remarkable as the oxygen measurements showed a continuum of values, implying a continuum degree of mixing between the two end members, the Loop Current waters and the southern GoM ones. Results from prior expeditions showed a gap in the oxygen content with almost no profiles with  $[O_2]^{UT}$  between 3 and 3.25 ml l<sup>-1</sup> (yellow stations being relatively rare), which led to the idea that the “gaps” at intermediate waters had to be filled mainly with unsampled northern GoM waters. 2015 was also distinctive for having a fairly extended LC to the northwest and by the detachment of several big LCEs: the Olympus eddy had detached two months prior to the cruise ( $a_{LCE} = 95\,516 \pm 4200$  km<sup>2</sup>), Nautilus ( $a_{LCE} = 51297 \pm 2500$  km<sup>2</sup>) and Michael ( $a_{LCE} = 55484 \pm 2800$  km<sup>2</sup>) up to 4 and 8 months before the cruise respectively, showing significant LCE activity prior to the expedition.

This situation changed the following year during the XIXIMI-5 cruise, when most of the stations in the central and western Gulf showed higher oxygen values and were considered as transition stations with  $[O_2]^{UT} > 2.75$  ml l<sup>-1</sup>. These results indicate that the transition and resident waters measured during the previous cruise had mixed to form a relatively well oxygenated and homogeneous water filling the main thermocline in the central GoM. Two months before this cruise, the LCE Poseidon ( $a_{LCE} = 98517 \pm 4900$  km<sup>2</sup>) detached from the LC, probably the largest LCE detachment recorded from January 2000 to this date. At the time of the cruise, it was still located near the LC and one CTD station sampled its center (Fig. 3). The oxygen profile of the LCE Poseidon was similar to the one from LCE Franklin measured by the ARGO float only showing deeper isopycnals (Table 3).



After the Poseidon detachment, there was a 19-month period without any detachments, while the 17 cm SSH contour of Poseidon was still visible in the western GoM 20 months after its detachment. The XIXIMI–6 cruise took place during August and September 2017, 18 months after the Poseidon detachment. During this cruise, most of the stations showed typical lower dissolved oxygen values of resident waters except for the LC ones. The homogeneously low  $[O_2]$  values measured during the XIXIMI–6 cruise could result from the mixing of the intermediate waters measured during XIXIMI–5, with the resident waters of the interior and by depletion of oxygen through respiration processes during a 19 month period without LCE detachment and no input of oxygen richer intermediate waters. Even the stations located over the remaining Poseidon LCE showed lower values of  $[O_2]^{UT} \leq 2.75 \text{ ml l}^{-1}$ . An implication of these observations is that although a huge LCE may still be visible with altimetry more than a year after its detachment (Meunier et al., 2018), their properties at depth, specifically  $[O_2]$  profiles, show clear signs of mixing with the Gulf's interior waters at these intermediate depths. Unfortunately, the arrival of a hurricane limited the sampling of seven of the planned stations in the  $25^\circ \text{ N}$  line. Probably some transition stations with higher  $[O_2]^{UT}$  could have been measured there, nonetheless, the remaining stations clustered around the typical low oxygen values of the interior waters.

295

The last cruise, XIXIMI–7, between May and June 2019, was also fraught by technical difficulties and was the least complete of all cruises. Fortunately, this time the  $25^\circ \text{ N}$  line was completed first, and although it shows four transition stations, the majority showed the typical oxygen concentration of GoM resident waters at depth. During this cruise, four stations were sampled in the western shelf, north of  $25^\circ \text{ N}$ , as part of a collaboration with other series of cruises. The LCE Revelle detached 10 months prior to this cruise ( $a_{LCE} = 78270 \pm 4000 \text{ km}^2$ ) and was still visible from altimetry data in the western GoM, but, again, as in the previous cruise, even stations located within this remanent eddy showed low oxygen content in the main thermocline waters. During the XIXIMI–6 and 7 cruises, one station in the northern shelf of the Mexican Caribbean was also sampled, with a profile fairly similar to the ones observed in the Yucatan Channel.

### 305 3.2 A decreasing trend in the detachment frequency of Loop Current Eddies

The time series of LCE detachments from 2000 to 2020 estimating the areas and dates of these events is shown in Fig. 4. These estimates were further compared with the ones reported by Hall and Leben (2016) and the names and dates given by the Woods Hole Eddies watch (<https://www.horizonmarine.com/loop-current-eddies>). Although there are some slight differences in the time of detachment, overall, the results from both identification exercises are fairly similar.

310 From January 2000 to December 2009 the estimated LCE shedding period was of one every  $5.85 \pm 2.60$  months or approximately two per year. In comparison, Vukovich (2012) estimated a frequency of  $8.8 \pm 5$  months per shedding during the 2000–2010 decade, the main difference being that in that study only the detachments of major rings were considered



(diameter > 300 km). The mean estimated diameter (assuming a circular shape) of the detached LCEs from 2000 to 2019 was  $272 \pm 12$  km, which falls close to previously reported diameters of approximately 300 km (Hall and Leben, 2016; Moreles et al., 2021). The maximum estimated diameter was from the LCE Poseidon of  $354 \pm 9$  km.

From January 2000 to December 2009 the average detached area was  $5.6 \pm 0.3 \cdot 10^4 \text{ km}^2$ , reaching a cumulative detached area during that decade of  $1.1 \pm 0.05 \cdot 10^6 \text{ km}^2$ . In comparison and following the same method and criteria, from January 2010 to December 2019 the estimated frequency was one detachment every  $8.4 \pm 4.9$  months, or 1.4 detachments per year, with an average area of  $5.7 \pm 0.3 \cdot 10^4 \text{ km}^2$ , making a cumulative detached area during that decade of  $0.8 \pm 0.04 \cdot 10^6 \text{ km}^2$  (Fig. 4). Although the average area during the 2010-2020 was slightly higher than during the previous decade, mainly because of two huge LCE detachments (Olympus and Poseidon), the important decrease in the detachment frequency was significant to make the total LCE area detached into the GoM waters during the 2000s decade almost double than the total area detached during the following decade. A decreasing trend in the number of LCE detachments during the last decade supports the hypothesis that a reduced transport of the LC, expected under some climate change scenarios, will decrease the frequency of LCE detachments (Moreles et al., 2021).

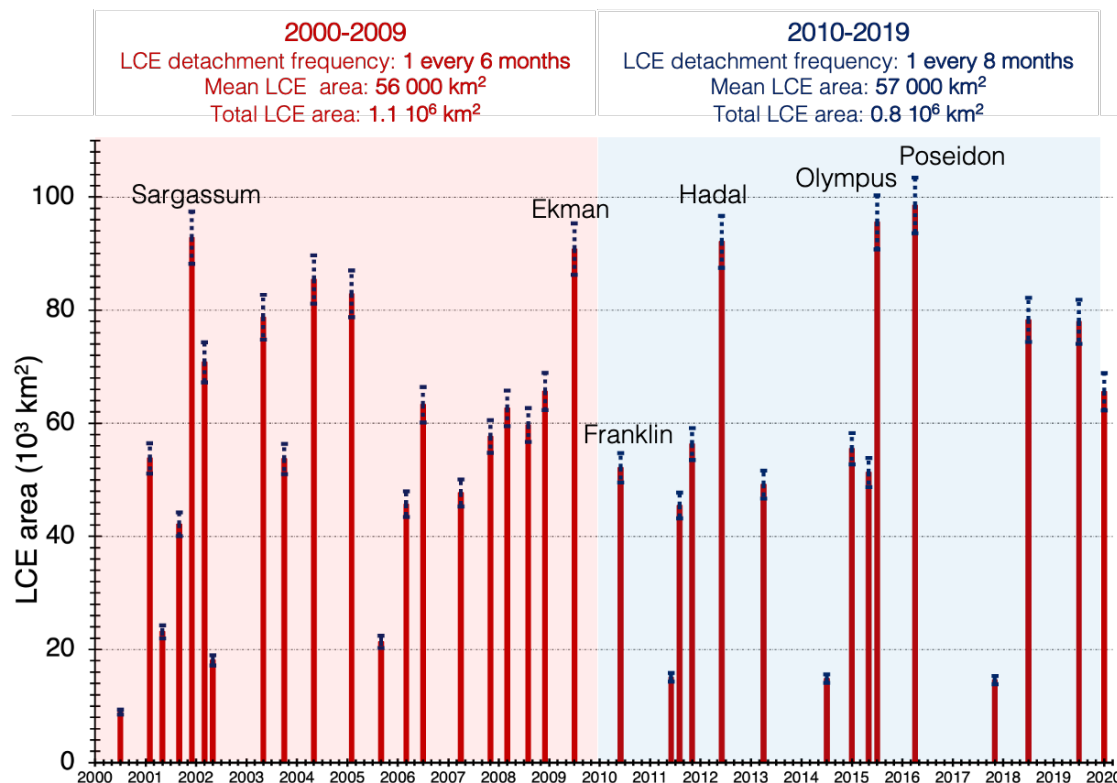
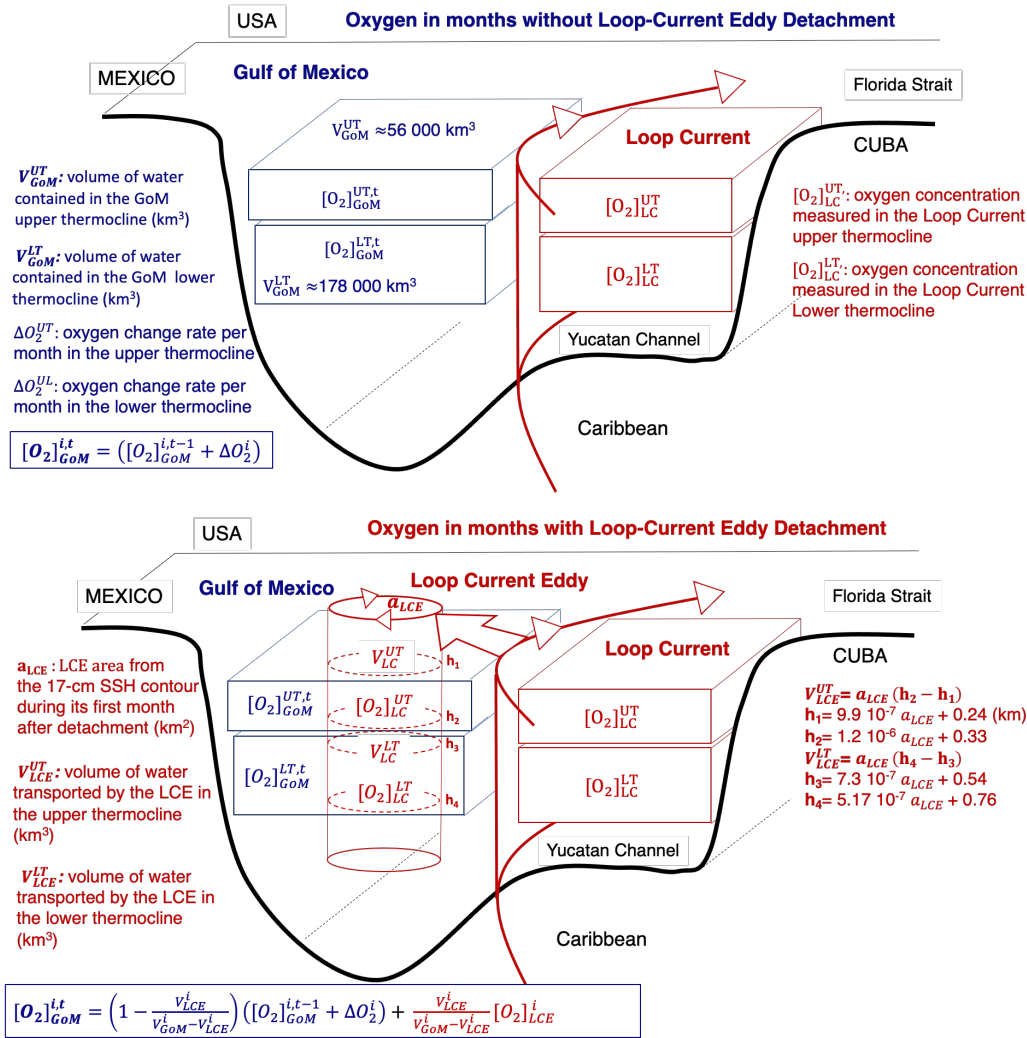


Figure 4. Date of detachment of Loop Current Eddies and their mean area (red bars) with standard deviation (blue dashed bars) estimated with the 17 cm SSH contour using AVISO altimetry. Information of relevant statistics to compare the decades as well as the name of relevant LCE names are presented as text.



### 3.3 Estimating oxygen content from LCE metrics



335 **Figure 5** Schematic representation of the box model equation and assumptions during (a) months without Loop Current Eddy detachment and (b) during months of Loop Current Eddy detachment.

In order to estimate how a decrease in the LCEs detachment frequency could affect the oxygen content of the GoM's main thermocline, a simple box model was formulated taking into account the input from the LCE detachments, following Eq. (1) schematized in Fig. 5:

$$[O_2]_{GoM}^{i,t} = \left(1 - \frac{V_{LCE}^i}{V_{GoM}^i - V_{LCE}^i}\right) ([O_2]_{GoM}^{i,t-1} + \Delta O_2^i) + \frac{V_{LCE}^i}{V_{GoM}^i - V_{LCE}^i} [O_2]_{LCE}^i \quad (1)$$





340 Where:

-  $[O_2]_{GoM}^{i,t}$  is the estimated oxygen content in the GoM main thermocline, for  $i=1$  the upper thermocline volume (with the isopycnal range  $\sigma_\theta$ : 26.3 to 26.6  $\text{kg m}^{-3}$ ) and for  $i=2$  the lower thermocline volume ( $\sigma_\theta$ : 27 to 27.25  $\text{kg m}^{-3}$ ),  $t$  is the time step with a time resolution of one month. The model starts at January 2000 with the initial values reported during that year,  $[O_2]_{GoM}^{1,1} = 3 \pm 0.2 \text{ ml l}^{-1}$  and  $[O_2]_{GoM}^{2,1} = 2.7 \pm 0.15 \text{ ml l}^{-1}$  (Jochens and DiMarco, 2008).

345 -  $V_{LCE}^i$  is the volume of water that enters the GoM in the upper or lower thermocline in the event of a LCE detachment during the month  $t$ . If no detachment was registered during the month  $t$ , then  $V_{LCE} = 0$  and the first term on the right side of the Eq. (1) is equal to 0, making Eq.1 a simple sum of the oxygen calculated the previous month plus the oxygen monthly change rate  $[O_2]_{GoM}^{i,t} = [O_2]_{GoM}^{i,t-1} + \Delta O_2^i$ . If a LCE detachment was registered during month  $t$ , then the transported LCE volume  $V_{LCE}^i$  for each thermocline layer is estimated from the LCE area (Fig. 4) during the first month after the detachment was registered. The volume of the LCEs upper and lower thermocline layers was estimated assuming that the eddies have a cylindrical shape with a constant area from the surface to the depths of the lower thermocline using Eq. (2):

$$- V_{LCE}^i = a_{LCE} (h_{n+1}^i - h_n^i) \quad (2)$$

Where  $a_{LCE}$  is the mean area of the LCE surface 17 cm SSH contour in  $\text{km}^2$  estimated during a month after its detachment was registered,  $h_1^i$  and  $h_2^i$  are the depths of the shallowest and deepest limits of the upper or lower thermocline layers in km. A cylindrical shape was chosen as the simplest shape to estimate the volume of water transported by an LCE of area  $a_{LCE}$ , but if the shape of the eddy was closer to a bowl rather than a cylinder, the volume of water transported by the LCE would be somewhat overestimated. The simple cylindrical shape is enough for the purposes and scope of this box model. To estimate the depths  $h_1^i$  and  $h_2^i$  a linear equation was calculated using the area of the detached LCEs Franklin and Poseidon and the depths of those isopycnals taken inside those LCEs with the data and equations shown in table 3.

360 -  $V_{GoM}^i$  is the approximate volume contained inside the deep GoM in the upper and lower thermocline. It was computed from the ETOPO1 bathymetry using the average depths of the isopycnals in the profiles from Gulf resident waters. For the upper thermocline the upper thermocline layer was estimated between  $155 \pm 7$  and  $210 \pm 8$  m, a depth range that according to the bathymetry contains a volume of  $V_{GoM}^{UT} = 56 \pm 7 \cdot 10^3 \text{ km}^3$ . For the lower thermocline layer, the average depths of the isopycnals were observed between  $345 \pm 20$  m to  $534 \pm 18$  m with an average volume of  $V_{GoM}^{LT} = 178 \pm 21 \cdot 10^3 \text{ km}^3$ .

365 These volumes are considered constant in the box model.

-  $[O_2]_{LCE}^i$  is the oxygen concentration in the volume of water  $V_{LCE}^i$  transported by the LCEs. We used the mean values measured with the BioARGO float and the XIXIMI cruises in the Caribbean and the LC with the highest standard deviation measured,  $[O_2]_{LCE}^{UT} = 3.5 \pm 0.12$  and  $[O_2]_{LCE}^{LT} = 2.7 \pm 0.15$ . Both values are considered constant from 2000 to 2019 with a relatively high standard deviation to encompass the full variability of this oxygen entrance. In the upper thermocline of the LC and the LCEs, measured values have remained fairly similar from 1980 to 2019 with a mean value of  $3.53 \pm 0.14 \text{ ml l}^{-1}$ ,



but in the lower thermocline the  $[O_2]$  seems to have decreased in the Caribbean and in the LC from  $3.05 \text{ ml l}^{-1}$  in 1980 (Morrison and Nowlin, 1977) to less than  $2.50 \text{ ml l}^{-1}$  in 2019. To simulate this oxygen variability, a mean value of  $2.70 \pm 0.25 \text{ ml l}^{-1}$  was chosen as the  $[O_2]$  entrance in the lower thermocline. If the oxygen input in the lower thermocline by LCE continues to drop, then the deoxygenation rate of the lower thermocline would be even higher than expected. This possibility is something to be aware of and might be addressed with further  $[O_2]$  measurements in the Cayman basin.

$\Delta O_2^i$  is the oxygen change rate in  $\text{ml l}^{-1} \text{ month}^{-1}$  in the upper and lower thermocline inside the GoM. This rate integrates an oxygen utilization rate (OUR) by biological respiration in the water column (Jenkins, 1992), as well as the oxygen lateral and vertical advection and diffusion terms (Oschlies et al., 2018). Each of these processes are complicated to measure explicitly, but the sum of its parts,  $\Delta O_2^i$ , was approximated by measuring the rate of  $[O_2]$  change during a period without LCE oxygen input. The mean  $[O_2]$  difference between stations in the approximate same coordinates (less than  $1^\circ$  of difference) between cruises XIXIMI-6 and XIXIMI-5, since they were the only consecutive cruises without any LCE detachments in between (Fig. 4). The estimated change rates are  $\Delta O_2^{UT} = -0.013 \pm 0.004 \text{ ml l}^{-1} \text{ month}^{-1}$  and  $\Delta O_2^{LT} = -0.0033 \pm 0.002 \text{ ml l}^{-1} \text{ month}^{-1}$ . Both oxygen change rates are negative, indicating that between August 2017 and June 2016, in the absence of LCE detachments, the sum of the biological consumption of oxygen and the vertical and horizontal oxygen mixing and diffusion resulted in a net loss of  $[O_2]$  in the GoM upper and lower thermocline. As the hypothesis of this work is that in the absence of LCEs the oxygen of the GoM main thermocline decreases, this change rate was considered to be constant from January 2000 to December 2019.

**Table 3**

Area and isopycnal depth of profiled Loop Current

Eddies and linear equations to relate both parameters

LCE	$a_{LCE}$ ( $\text{km}^2$ )	$\sigma_\theta$ ( $\text{kg m}^{-3}$ )	Depth (km)
		26.3	<b>0.296</b>
<b>Franklin</b> 13 jun 2010 Bio ARGO Profile 1	<b>52 133</b> $\pm$ 2 870	26.6 27	<b>0.389</b> <b>0.579</b>
		27.15	<b>0.769</b>
		26.3	<b>0.341</b>
<b>Poseidon</b> 18 june 2016 XIXIMI-5 Profile B37	<b>98 516</b> $\pm$ 4 955	26.6 27	<b>0.445</b> <b>0.613</b>
		27.15	<b>0.812</b>
	26.3	$h_1 = 9.9 \cdot 10^{-7} a_{LCE} + 0.24$	





$$26.6 \quad h_2 = 1.2 \cdot 10^{-6} a_{LCE} + 0.33$$

$$27 \quad h_3 = 7.3 \cdot 10^{-7} a_{LCE} + 0.54$$

$$27.15 \quad h_4 = 5.17 \cdot 10^{-7} a_{LCE} + 0.76$$

---

\* ± of slope and intercept not shown

390 It is certain that the oxygen change rates in the thermocline will vary monthly and annually just as the OUR varies too (Jenkins  
et al., 1982) as a result of the seasonal variability of productivity and organic matter export from the surface (Damien et al.,  
2018), and even as a result of the same mesoscale eddies that can influence the surface productivity (McGillicuddy et al.,  
1998). Furthermore, the vertical advection and diffusion terms can vary at different scales and might be affected by the  
mesoscale circulation too (Damien et al., 2021). However, since the measurements were taken with a yearly resolution at  
maximum, there is no information on the seasonal timescale or higher frequency variability of these oxygen consumption  
395 processes.

Another main simplification of this model is the assumption that the LCE oxygen content mixes immediately with the GoM  
oxygen content within the first month of the eddy detachment. This is obviously not the case, as it was observed during the  
XIXIMI-3 cruise, eddies maintain, to some extent, coherence and their internal properties for a few months or in some cases  
400 even more than a year after detachment (Meunier et al., 2020). Nevertheless, even if the oxygen content of the LCE is slowly  
mixed with the GoM resident waters, the long-term concentrations would not change, since the changes in oxygen content  
in the GoM would still be pondered by the LCE and GoM volume ratio and reduced by the oxygen change rate inside the  
basin.

405 To represent part of the real variability of the system that can't be resolved with the crude approximations used in this simple  
parametrization, the model was ran using a combination of the mean, max (mean plus standard deviation) and min (mean  
minus standard deviation) values of each of its parameters to estimate the following scenarios:

- The mean scenario, using the mean values of each parameter, represented as the solid blue and red lines for the upper and  
lower thermocline respectively in Fig. 6.
- 410 - The maximum scenario, with a maximum [O<sub>2</sub>] entrance during a LCE detachment and a maximum [O<sub>2</sub>] change rate inside  
the Gulf, using max LCEs volumes, min GoM volumes, max [O<sub>2</sub>] transported by LCEs, max initial [O<sub>2</sub>] inside the GoM and  
max absolute oxygen change rate inside the GoM (dashed blue and red lines in Fig. 6).
- The minimum scenario, with a minimum [O<sub>2</sub>] entrance during a LCE detachment and minimum [O<sub>2</sub>] change rate inside the  
Gulf, using min LCEs volumes, max GoM volumes, min [O<sub>2</sub>] transported by LCEs, min initial [O<sub>2</sub>] inside the GoM and min  
415 absolute oxygen change rate inside the GoM (dotted blue and red lines in Fig. 6).



**Table 4**

List of parameters, equations and assumptions used for the box model.

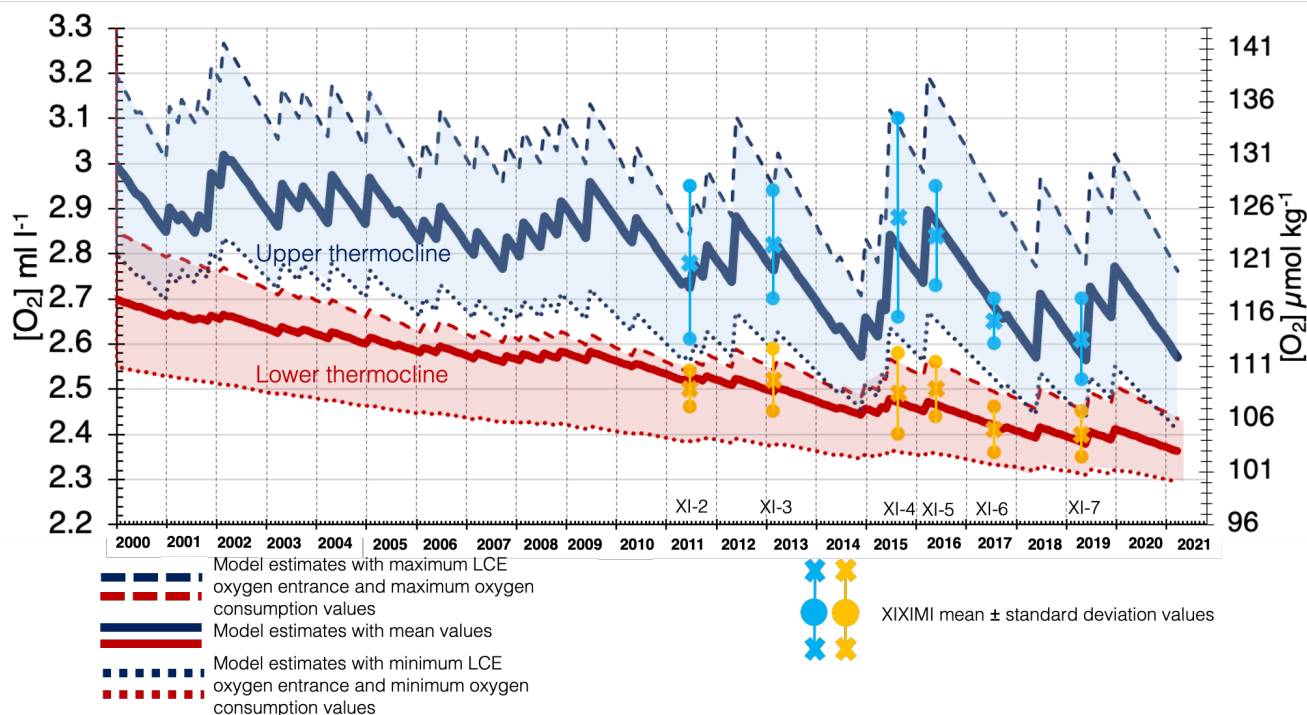
Parameter	Values		Assumptions and references
	$\sigma_{\theta}$ (kg m <sup>-3</sup> ) i = 1: 26.3-26.6	$\sigma_{\theta}$ i = 2: 27-27.25	
<b>V<sub>GoM</sub>:</b> Volume of water inside the GoM in the density range	<b>56 ± 7 10<sup>3</sup></b> (km <sup>3</sup> ) 161 to 205 m	<b>178 ± 21 10<sup>3</sup></b> (km <sup>3</sup> ) 353 to 506 m	Calculated from ETOPO1 bathymetry data assuming a constant depth for each isopycnal inside the GoM.
<b>a<sub>LCE</sub>:</b> Loop-Current Eddy Area and detachment date	Estimated from the 17-cm contour not connected to the Loop-Current, without reconnection in the following month and without diameter restriction.		Using AVISO altimetry data, following Leben <i>et al.</i> , 2015.
<b>V<sub>LCE</sub>:</b> Volume of water transported by LCEs	<b>a<sub>LCE</sub> (h<sub>2</sub>-h<sub>1</sub>)</b>	<b>a<sub>LCE</sub> (h<sub>4</sub>-h<sub>3</sub>)</b>	Estimated assuming a cylindrical shape. This volume is assumed to mix diapycnally with the GoM volume and immediately after the LCE detachment month.
<b>h:</b> Depth of isopycnals inside LCEs	<b>h<sub>1</sub></b> ( $\sigma_{\theta}$ = 26.3) 9.0 10 <sup>-7</sup> A + 0.24 <b>h<sub>2</sub></b> ( $\sigma_{\theta}$ = 26.6) 1.8 10 <sup>-6</sup> A + 0.33	<b>h<sub>3</sub></b> ( $\sigma_{\theta}$ = 27) 6.7 10 <sup>-7</sup> A + 0.54 <b>h<sub>4</sub></b> ( $\sigma_{\theta}$ = 27.25) - 3.14 10 <sup>-7</sup> A + 0.80	Using a linear regression from the area of LCE Franklin (June 2010) and density-depth profile from Bio Argo Buoy and the area of LCE Poseidon (Apr 2016) and profile B <sub>37</sub> from cruise XI-5 (table 3).
<b>[O<sub>2</sub>]<sub>LCE</sub>:</b> [O <sub>2</sub> ] transported by LCEs	<b>3.5 ± 0.12</b> ml l <sup>-1</sup> 152.3 ± 5.2 μmol kg <sup>-1</sup>	<b>2.7 ± 0.15</b> ml l <sup>-1</sup> 117.4 ± 6.2 μmol kg <sup>-1</sup>	Constant, from measurements in the Loop Current and in the Caribbean (this study, Morrison and Nowlin, 1977, Rivas <i>et al.</i> , 2005).
<b>ΔO<sub>2</sub>:</b> [O <sub>2</sub> ] change rate inside the GoM	<b>- 0.16 ± 0.05</b> ml l <sup>-1</sup> yr <sup>-1</sup> -6.7 ± 2.2 μmol kg <sup>-1</sup> yr <sup>-1</sup>	<b>- 0.04 ± 0.02</b> ml l <sup>-1</sup> yr <sup>-1</sup> -1.7 ± 0.9 μmol kg <sup>-1</sup> yr <sup>-1</sup>	Constant, estimated from the measured decrease during a period of no LCEs detachment (June 2016 - Aug 2017). Here as per year for an easier comparison with reported OUR values elsewhere.
Starts at t = 1: Jan 2000	<b>[O<sub>2</sub>]<sup>UT,1</sup> = 3.0 ± 0.2</b> ml l <sup>-1</sup> 130.5 ± 8.7 μmol kg <sup>-1</sup>	<b>[O<sub>2</sub>]<sup>LT,1</sup> = 2.7 ± 0.15</b> ml l <sup>-1</sup> 117.4 ± 6.2 μmol kg <sup>-1</sup>	LCE separation date is estimated within one month, so the model uses a one month time lapse. Starting with values from Jochens and DiMarco, (2008)

**Equation**

$$[O_2]_{GoM}^{i,t} = \frac{V_{LCE}^i}{V_{GoM}^i - V_{LCE}^i} [O_2]_{LCE}^i + \left(1 - \frac{V_{LCE}^i}{V_{GoM}^i - V_{LCE}^i}\right) ([O_2]_{GoM}^{i,t-1} + \Delta O_2^i)$$



To compare the model estimations with the actual measurements, the mean and standard deviation measured  $[O_2]$  in each XIXIMI cruise are represented as colored X and error bars in Fig. 6. Most of the XIXIMI measurements enter inside the model shading, except for the XIXIMI-4 large  $[O_2]$  variability in both the upper and lower main thermocline that isn't well represented. It could be that the model doesn't represent well the periods of high  $[O_2]$  heterogeneity produced probably during periods of important LCE activity as seen during XIXIMI-4, but represents correctly the mix and homogenization of oxygen during periods of low LCE activity. The mean  $[O_2]$  measured during XIXIMI-6 and 7 in the upper thermocline layer is closer to the minimum  $[O_2]$  entrance and minimum  $[O_2]$  change rate scenario than to the maximum scenario. As such it can be interpreted that, at least, between 2017 to 2019 the oxygen input via LCE detachment was closer to the lower estimates and/or that the rate of  $[O_2]$  change rate was lower (higher decrease rate) than previously estimated. In any case, more measurements are needed in order to confirm the persistence of this trend towards lower oxygen concentration values in the GoM main thermocline. If the basic assumptions that support this simple model are found sound it may provide a useful first approximation tool to estimate the oxygen level conditions in the main thermocline of the GoM by keeping track of the LCE metrics via altimetry products.



430

Figure 6. Oxygen variability estimated from box model for the upper (blue) and lower (red) thermocline from 2000 to 2020.

With the parameters used in the model (Table 4), the following estimations were made:

-The average LCE area threshold to maintain constant oxygen concentration levels in the upper and lower thermocline at 2.60 and 2.40  $ml\ l^{-1}$  respectively would be 74000  $km^2$  per year for the upper thermocline and 93000  $km^2$  per year for the

435



lower thermocline. An average LCE detachment area of 93000 km<sup>2</sup> per year would bring the upper thermocline oxygen concentration to 2.90 ml l<sup>-1</sup> (inside the concentration ranges measured in 2000, Table 1).

- An average LCE area of 80000 km<sup>2</sup> per year as measured during the 2010-2020 decade (Fig. 4), would bring the average [O<sub>2</sub>] to 2.7 and 2.35 ml l<sup>-1</sup> in the upper and lower thermocline respectively.

440 - If, over the 2020-2030 decade, the average LCE area decreases below 70000 km<sup>2</sup> per year, the average upper and lower thermocline oxygen concentrations would fall below 2.5 and 2.3 ml l<sup>-1</sup> respectively.

### 3.3 Global and future trends

A possible LC slow-down has been hypothesized in global warming scenarios (Liu et al., 2012; Rhein et al., 2011). Some  
445 model studies suggest that high (low) Yucatan current transports imply deeper (weaker) LC extension into the GoM (Chang and Oey, 2012). Others find modifications in the LC behavior related to changes in the model stratification (Moreles et al., 2021) that might explain the observed decrease in the LCE detachment frequency. Both explain their model behavior using the mechanism suggested by Pichevin and Nof (1997). Although the occasionally detached eddies might be getting larger, the total detached volume per year seems to have decreased during the last decade.

450

Hence, the number LCEs entering the GoM seems to be a key process for the ventilation of its main thermocline, implying that a decrease in the detachment of eddies from the LC would most likely lead to a deoxygenation trend in the GoM interior thermocline water masses. Observations (Athié et al., 2012; 2020; Sheinbaum et al., 2016; Hamilton et al., 2018) suggest a more complicated behavior involving full depth ocean processes not only at the upper layer, and indicate there is not a simple  
455 and straightforward relation between LC transport and extension.

In any case, if a connection can be established between the large scale circulation and the LC and its eddy shedding (Sturges et al., 2009), a weakening of the Gulf stream that has been suggested by some studies in connection with changes in the Atlantic Meridional Overturning Circulation (AMOC, Chen et al., 2019; Rahmstorf et al., 2015; Caesar et al., 2018; Smeed  
460 et al., 2018) may cause a reduction in the LCE shedding frequency. If such a connection does indeed exist, then a continuous weakening of the AMOC may lead to a deoxygenation trend of the main thermocline waters of the GoM in the future. On the other hand, if such connection indeed exists, measuring a deoxygenation trend in the GoM can be used as a proxy to estimate the AMOC weakening, a task perhaps easier to carry out given the semi-enclosed characteristics of the GoM. The road to stablish such kind of connections is paved with large uncertainties but it is certainly a venue worthy of further  
465 exploration.



#### 470 4 Conclusions

Historical and new data presented here suggest a deoxygenation trend in the main thermocline of the GoM, thereby increasing the volume of hypoxic waters that might affect the deep-water ecosystems in the main thermocline of the GoM and its margins. The time series obtained from six cruises in the deep-water region of the GoM illustrates the spatial and temporal  
475 variability of  $[O_2]$  and the links between the oxygen concentrations in the upper and lower main thermocline waters and the detachment frequency and volumes of LCEs that enter the GoM proper.

The time series obtained from six oceanographic cruises, from 2010 to 2019, show evidence that LCEs entering the GoM transport significant volumes of relatively oxygen rich waters into the Gulf's interior, thereby ventilating the main  
480 thermocline waters of the basin. Observations from measurements after a high LCE activity period show a relatively well-ventilated main thermocline, with oxygen values above  $2.8 \text{ ml l}^{-1}$  in the upper thermocline. In contrast, measurements taken after periods of more than a year with no LCE detachment consistently show an important oxygen decrease of its main thermocline waters.

485 According to AVISO altimetry data, during the 2000–2010 decade the average detachment frequency was one LCE every 6 months with an average detached area of  $110\,000 \text{ km}^2$  per year. In contrast, during the 2010–2020 decade, the average detachment frequency was one LCE every 8 months with an average detached area of  $80\,000 \text{ km}^2$  per year. Although the biggest LCEs were measured in 2015 and 2016, this did not compensate the lower frequency of detachments that almost halved the total LCE area detached per year.

490 Using the oxygen and altimetry measurements a series of parameters were selected to formulate a simple box model to reproduce the  $[O_2]$  temporal variability in the GoM main thermocline. Using the box model parameters, it was estimated that an average total area of about  $93\,000 \text{ km}^2$  per year is necessary to maintain the oxygen levels of the main thermocline constant within the GoM.

495 These results imply that a further decrease in the LCE detachment frequency could lead to a more severe deoxygenation of the GoM main thermocline waters. The accessibility of altimetry data makes it fairly simple to monitor this behavior in the future in order to predict oxygen concentrations of GoM main thermocline waters. Although the uncertainties in the model warrant the need to continue gathering more in situ data in the deep-water region of the GoM, a task that could be fulfilled  
500 deploying more BioARGO floats within the GoM. A possible link between the weakening of the AMOC and the deoxygenation trend of the main thermocline waters of the GoM suggests important implications for the ecological web structure at these depths and its long-term sustainability. Such a link remains to be established, but if it were verified, the



number of detached eddies and the flow through the Yucatan Channel could serve as a proxy to estimate the level of AMOC weakening using further GoM oxygen measurements.

505

**Data availability:** Supplementary data to this article can be found online at <https://doi.org/10.5281/zenodo.7830465>

**Author contributions:** JQ, JCH, and JS conceptualized the analysis and developed the methodology. JQ did the formal analysis and developed the numerical simulation. JQ did the writing and original draft preparation. All authors provided feedback on the analysis and interpretation of results and contributed to reviewing and editing the manuscript. JCH acquired funding of this research. All authors have read and agreed to the published version of the manuscript.

510

**Competing interests:** The authors declare that they have no conflict of interest.

**Acknowledgements.** We acknowledge Enric Pallàs, Pierre Damien and Helmut Maske for the important feedback they provided. We mainly want to acknowledge Vicente Ferreira whose observations and understanding made this paper possible. Finally thanks to the CONACYT, CICESE and CiGOM for their financial support.

515

Financial support: Research funded by the National Council of Sciences and Technology of Mexico - Secretariat of Energy - Hydrocarbons Trust Project 201441. This is a contribution of the Gulf of Mexico Research Consortium (CiGOM)

520

## References

Andrews, O., Buitenhuis, E., Le Quéré, C., and Suntharalingam, P.: Biogeochemical modelling of dissolved oxygen in a changing ocean, *Philos. T. R. Soc. A.*, 375, <https://doi.org/10.1098/rsta.2016.0328>, 2017.

525

Athié, G., Candela, J., Ochoa, J., and Sheinbaum, J.: Impact of Caribbean cyclones on the detachment of Loop Current anticyclones, *J. Geophys. Res–Oceans.*, 117, C3018, <https://doi.org/10.1029/2011JC007090>, 2012.

Athié, G., Sheinbaum, J., Candela, J., Ochoa, J., Pérez-Brunius, P., and Romero-Arteaga, A.: Seasonal variability of the transport through the Yucatan Channel from observations, *J. Phys. Oceanogr.*, 50, 343–360, <https://doi.org/10.1175/JPO-D-18-0269.1>, 2020.

530

Billheimer, S. J., Talley, L. D., and Martz, T. R.: Oxygen seasonality, utilization rate, and impacts of vertical mixing in the Eighteen Degree Water region of the Sargasso Sea as observed by profiling biogeochemical floats, *Global Biogeochem. Cy.*, 35, e2020GB006824, <https://doi.org/10.1029/2020GB006824>, 2021.

535



Brandt, P., Bange, H. W., Banyte, D., Dengler, M., Didwischus, S.-H., Fischer, T., Greatbatch, R. J., Hahn, J., Kanzow, T., Karstensen, J., Körtzinger, A., Krahnemann, G., Schmidtko, S., Stramma, L., Tanhua, T., and Visbeck, M.: On the role of circulation and mixing in the ventilation of oxygen minimum zones with a focus on the eastern tropical North Atlantic, *Biogeosciences*, 12, 489–512, <https://doi.org/10.5194/bg-12-489-2015>, 2015.

Bushinsky, S.M., Emerson, S.R., Riser, S.C., and Swift, D.D.: Accurate oxygen measurements on modified Argo floats using in situ air calibrations, *Limnol. Oceanogr-Meth*, 14, 491–505, <https://doi.org/10.1002/lom3.101076>, 2016.

Caesar, L., Rahmstorf, S., Robinson, A., Feulner, G., and Saba, V.: Observed fingerprint of a weakening Atlantic Ocean overturning circulation, *Nature*, 556, 191–196, <https://doi.org/10.1038/s41586-018-0006-5>, 2018.

Carrillo, L., Johns, E. M., Smith, R. H., Lamkin, J. T., and Largier, J. L.: Pathways and hydrography in the Mesoamerican Barrier Reef System Part 2: Water masses and thermohaline structure, *Cont. Shelf. Res.*, 120, 41–58, <https://doi.org/10.1016/j.csr.2016.03.014>, 2016.

Chang, Y. L., and Oey, L. Y.: Why does the Loop Current tend to shed more eddies in summer and winter?, *Geophys. Res. Lett.*, 39, <https://doi.org/10.1029/2011GL050773>, 2012.

Chen, C., Wang, G., Xie, S.P., and Liu, W.: Why does global warming weaken the Gulf Stream but intensify the Kuroshio?, *J. Climate*, 32, 7437–7451, <https://doi.org/10.1175/JCLI-D-18-0895.1>, 2019.

Damien, P., Pasqueron de Fommervault, O., Sheinbaum, J., Jouanno, J., Camacho-Ibar, V. F., and Duteil, O.: Partitioning of the open waters of the Gulf of Mexico based on the seasonal and interannual variability of chlorophyll concentration, *J. Geophys. Res-Oceans.*, 123, 2592–2614, <https://doi.org/10.1002/2017JC013456>, 2018.

Damien, P., Sheinbaum, J., Pasqueron de Fommervault, O., Jouanno, J., Linacre, L., and Duteil, O.: Do Loop Current eddies stimulate productivity in the Gulf of Mexico?, *Biogeosciences*, 18, 4281–4303, <https://doi.org/10.5194/bg-18-4281-2021>, 2021.

Elliott, B.A.: Anticyclonic rings in the Gulf of Mexico, *J. Phys. Oceanogr.*, 12, 1292–1309, [https://doi.org/10.1175/1520-0485\(1982\)012<1292:ARITGO>2.0.CO;2](https://doi.org/10.1175/1520-0485(1982)012<1292:ARITGO>2.0.CO;2), 1982.





- 570 Falkowski, P. G., Algeo, T., Codispoti, L., Deutsch, C., Emerson, S., Hales, B., Huey, R. B., Jenkins, W. J., Kump, L. R., Levin, L. A., Lyons, T. W., Nelson, N. B., Schofield, O. S., Summons, R., Talley, L. D., Thomas, E., Whitney, F., and Pilcher, C. B.: Ocean deoxygenation: past, present, and future, *Eos, Trans. Am. Geophys. Union.*, 92, 409–410, <https://doi.org/10.1029/2011EO460001>, 2011.
- 575 Furuya, K., and Harada, K.: An automated precise Winkler titration for determining dissolved oxygen on board ship, *J. Oceanogr.*, 51, 375–383, <https://doi.org/10.1007/BF02285173>, 1995.
- Gruber, N., Doney, S. C., Emerson, S. R., Gilbert, D., Kobayashi, T., Körtzinger, A., Johnson, G. C., Johnson, K. S., Riser, S. C., and Ulloa, O.: Adding oxygen to ARGO: developing a global in situ observatory for ocean deoxygenation and  
580 biogeochemistry, in: *Proceedings of Oceanobs'09: Sustained Ocean Observations and Information for Society*, Venice, Italy, 21–25 September 2009, 21–25, <https://doi.org/10.5270/OceanObs09.cwp.39>, 2010.
- Hall, C. A., and Leben, R. R.: Observational evidence of seasonality in the timing of loop current eddy separation, *Dynam. Atmos. Oceans*, 76, 240–267, <https://doi.org/10.1016/j.dynatmoce.2016.06.002>, 2016.  
585
- Hahn, J., Brandt, P., Schmidtke, S., and Krahnemann, G.: Decadal oxygen change in the eastern tropical North Atlantic, *Ocean Sci.*, 13, 551–576, <https://doi.org/10.5194/os-13-551-2017>, 2017.
- Hamilton, P., Leben, R., Bower, A., Furey, H., and Pérez–Brunius, P.: Hydrography of the Gulf of Mexico using autonomous  
590 floats, *J. Phys. Oceanogr.*, 48, 773–794, <https://doi.org/10.1175/JPO–D–17–0205.1>, 2018.
- Hurlburt, H. E., and Thompson, J. D.: A numerical study of Loop Current intrusions and eddy shedding, *J. Phys. Oceanogr.*, 10, 1611–1651, [https://doi.org/10.1175/1520-0485\(1980\)010<1611:ANSOLC>2.0.CO;2](https://doi.org/10.1175/1520-0485(1980)010<1611:ANSOLC>2.0.CO;2), 1980.
- 595 Jenkins, W. J.: Oxygen utilization rates in North Atlantic subtropical gyre and primary production in oligotrophic systems, *Nature*, 300, 246–248, <https://doi.org/10.1038/300246a0>, 1982.
- Jochens, A. E., Bender, L. C., DiMarco, S. F., Morse, J. W., Kennicutt II, M. C., Howard, M. K., and Nowlin, Jr., W. D.: Understanding the Processes that Maintain the Oxygen Levels in the Deep Gulf of Mexico: Synthesis Report, U.S.  
600 Department of the Interior, Minerals Management Service, Gulf of Mexico OCS Region, New Orleans, LA. OCS Study MMS 2005–032. 142 pp, 2005.



- Jochens, A. E., and DiMarco, S. F.: Physical oceanographic conditions in the deepwater Gulf of Mexico in summer 2000–2002, *Deep–Sea Res. Pt. II*, 55, 2541–2554, <https://doi.org/10.1016/j.dsr2.2008.07.003>, 2008.
- 605
- Kinard, W. F., Atwood, D. K., and Giese, G. S.: Dissolved oxygen as evidence for 18 C Sargasso Sea Water in the eastern Caribbean Sea, *Deep Sea Research and Oceanographic Abstracts*, 21, 79–82, [https://doi.org/10.1016/0011-7471\(74\)90021-7](https://doi.org/10.1016/0011-7471(74)90021-7), 1974.
- 610
- Kwon, Y. O., and Riser, S. C.: North Atlantic subtropical mode water: A history of ocean–atmosphere interaction 1961–2000, *Geophys. Res. Lett.*, 31, L19307, <https://doi.org/10.1029/2004GL021116>, 2004.
- Leben, R. R.: Altimeter–derived loop current metrics, *Geoph. Monog. Series*, 161, 181–201, <https://doi.org/10.1029/161GM15>, 2005.
- 615
- Levin, L. A.: Manifestation, drivers, and emergence of open ocean deoxygenation, *Annu. Rev. Mar. Sci.*, 10, 229–260, <https://doi.org/10.1146/annurev-marine-121916-063359>, 2018.
- Liu, Y., Lee, S.-K., Muhling, B. A., Lamkin, J. T., and Enfield, D. B.: Significant reduction of the Loop Current in the 21st century and its impact on the Gulf of Mexico, *J. Geophys. Res–Oceans.*, 117, C05039, <https://doi.org/10.1029/2011JC007555>, 2012.
- 620
- Maul, G. A.: The annual cycle of the Gulf Loop Current Part I: Observations during a one–year time series, in: *Collected reprints, Atlantic Oceanographic and Meteorological Laboratories, U.S. Department of Commerce, National Oceanic and Atmospheric Administration, Environmental Research Laboratories, Boulder, Colorado*, 1, 398–416, 1977.
- 625
- Maul, G. A.: The 1972–1973 cycle op the Golf Loop Current Part II: mass and salt balances of the basin, in: *Collected reprints, Atlantic Oceanographic and Meteorological Laboratories, U.S. Department of Commerce, National Oceanic and Atmospheric Administration, Environmental Research Laboratories, Boulder, Colorado*, 358–380, 1980.
- 630
- Maul, G. A., and Vukovich, F. M.: The relationship between variations in the Gulf of Mexico Loop Current and Straits of Florida volume transport, *J. Phys. Oceanogr.*, 23, 785–796, [https://doi.org/10.1175/1520-0485\(1993\)023<0785:TRBVIT>2.0.CO;2](https://doi.org/10.1175/1520-0485(1993)023<0785:TRBVIT>2.0.CO;2), 1993.
- 635
- McDougall, T. J., and Barker, P. M.: *Getting started with TEOS–10 and the Gibbs Seawater (GSW) oceanographic toolbox, SCOR/IAPSO WG127*, 28 pp, ISBN 9780646556215, 2011.



- 640 McGillicuddy Jr., D. J., Robinson, A. R., Siegel, D. A., Jannasch, H. W., Johnson, R., Dickey, T. D., McNeil, J., Michaels, A. F., and Knap, A. H.: Influence of mesoscale eddies on new production in the Sargasso Sea, *Nature*, 394, 263–266, <https://doi.org/10.1038/28367>, 1998.
- Meunier, T., Pallás-Sanz, E., Tenreiro, M., Portela, E., Ochoa, J., Ruiz-Angulo, A., and Cusí, S.: The vertical structure of a Loop Current Eddy, *J. Geophys. Res–Oceans.*, 123, 6070–6090, <https://doi.org/10.1029/2018JC013801>, 2018.
- 645 Meunier, T., Sheinbaum, J., Pallás-Sanz, E., Tenreiro, M., Ochoa, J., Ruiz-Angulo, A., Carton, X., and de Marez, C.: Heat content anomaly and decay of warm-core rings: The case of the Gulf of Mexico, *Geophys. Res. Lett.*, 47, e2019GL085600, <https://doi.org/10.1029/2019GL085600>, 2020.
- Moreles, E., Zavala-Hidalgo, J., Martínez-López, B., and Ruiz-Angulo, A.: Influence of stratification and Yucatan Current transport on the Loop Current Eddy shedding process, *J. Geophys. Res–Oceans.*, 126, e2020JC016315, <https://doi.org/10.1029/2020JC016315>, 2021.
- 650 Morrison, J. M., and Nowlin Jr, W. D.: Repeated nutrient, oxygen, and density sections through the Loop Current, *J. Mar. Res.*, 35, 105–128, 1977.
- 655 Morrison, J. M., Merrell Jr., W. J., Key, R. M., and Key, T. C.: Property distributions and deep chemical measurements within the western Gulf of Mexico, *J. Geophys. Res–Oceans.*, 88, 2601–2608, <https://doi.org/10.1029/JC088iC04p02601>, 1983.
- 660 Oschlies, A., Brandt, P., Stramma, L., and Schmidtko, S.: Drivers and mechanisms of ocean deoxygenation, *Nat. Geosci.*, 11, 467–473, <https://doi.org/10.1038/s41561-018-0152-2>, 2018.
- Pichevin, T., and Nof, D.: The eddy cannon, *Ocean. Lit. Rev.*, 5, 415, [https://doi.org/10.1016/S0967-0637\(96\)00064-7](https://doi.org/10.1016/S0967-0637(96)00064-7), 1997.
- 665 Pitcher, G. C., Aguirre–Velarde, A., Breitburg, D., Cardich, J., Carstensen, J., Conley, D. J., Dewitte, B., Engel, A., Espinoza–Morriberón, D., Flores, G., Garçon, V., Graco, M., Grégoire, M., Gutiérrez, D., Martin Hernandez–Ayón, J., May Huang, H., Isensee, K., Elena, J. M., Levin, L., Lorenzo, A., Machu, E., Merma, L., Montes, I., Swa, N., Paulmier, A., Roman, M., Rose, K., Hood, R., Rabalais, N. N., Gro, V. S. A., Salvattecchi, R., Sánchez, S., Sifeddine, A., Wahab Tall, A., Van Der Plas, A. K., Yasuhara, M., Zhang, J., and Zhu, Z.: System controls of coastal and open ocean oxygen depletion, *Prog. Oceanogr.*, 670 197, 102613, <https://doi.org/10.1016/j.pocean.2021.102613>, 2021.



- Portela, E., Tenreiro, M., Pallàs-Sanz, E., Meunier, T., Ruiz-Angulo, A., Sosa-Gutiérrez, R., and Cusí, S.: Hydrography of the central and western Gulf of Mexico, *J. Geophys. Res–Oceans.*, 123, 5134–5149, <https://doi.org/10.1029/2018JC013813>, 2018.
- 675
- Portela, E., Kolodziejczyk, N., Vic, C., and Thierry, V.: Physical mechanisms driving oxygen subduction in the global ocean, *Geophys. Res. Lett.*, 47, e2020GL089040, <https://doi.org/10.1029/2020GL089040>, 2020.
- Rabalais, N. N., Turner, R. E., and Wiseman Jr, W. J.: Gulf of Mexico hypoxia, aka “The dead zone”, *Annu. Rev. Ecol. and Syst.*, 33, 235–263, <https://doi.org/10.1146/annurev.ecolsys.33.010802.150513>, 2002.
- 680
- Rahmstorf, S., Box, J.E., Feulner, G., Mann, M.E., Robinson, A., Rutherford, S., and Schaffernicht, E.J.: Exceptional twentieth-century slowdown in Atlantic Ocean overturning circulation, *Nat. Clim. Change*, 5, 475–480, <https://doi.org/10.1038/NCLIMATE2554>, 2015.
- 685
- Rhein, M., Kieke, D., HuttI-Kabus, S., Roessler, A., Mertens, C., Meissner, R., Klein, B., Boning, C. W., and Yashayaev, I.: Deep water formation, the subpolar gyre, and the meridional overturning circulation in the subpolar North Atlantic, *Deep-Sea Res.*, 58, 1819–1832, <https://doi.org/10.1016/j.dsr2.2010.10.061>, 2011.
- Rivas, D., Badan, A., and Ochoa, J.: The ventilation of the deep Gulf of Mexico, *J. Phys. Oceanogr.*, 35, 1763–1781, <https://doi.org/10.1175/JPO2786.1>, 2005.
- 690
- Robbins, P. E., Price, J. F., Owens, W. B., and Jenkins, W. J.: The importance of lateral diffusion for the ventilation of the lower thermocline in the subtropical North Atlantic, *J. Phys. Oceanogr.*, 30, 67–89, [https://doi.org/10.1175/1520-0485\(2000\)030<0067:TIOLDF>2.0.CO;2](https://doi.org/10.1175/1520-0485(2000)030<0067:TIOLDF>2.0.CO;2), 2000.
- 695
- Sheinbaum, J., Athié, G., Candela, J., Ochoa, J., and Romero-Arteaga, A.: Structure and variability of the Yucatan and loop currents along the slope and shelf break of the Yucatan channel and Campeche bank, *Dynam. Atmos. Oceans.*, 76, 217–239, <https://doi.org/10.1016/j.dynatmoce.2016.08.001>, 2016.
- 700
- Smeed, D. A., Josey, S. A., Beaulieu, C., Johns, W. E., Moat, B. I., Frajka-Williams, E., Rayner, D., Meinen, C. S., Baringer, M. O., Bryden, H. L., and McCarthy, G. D.: The North Atlantic Ocean is in a state of reduced overturning, *Geophys. Res. Lett.*, 45, 1527–1533, <https://doi.org/10.1002/2017GL076350>, 2018.



705 Stramma, L., Schmidtko, S., Levin, L.A., and Johnson, G.C.: Ocean oxygen minima expansions and their biological impacts, *Deep-Sea Res. Pt. I.*, 57, 587–595, <https://doi.org/10.1016/j.dsr.2010.01.005>, 2010.

Sturges, W., Hoffmann, N. G., and Leben, R. R.: A trigger mechanism for Loop Current ring separations, *J. Phys. Oceanogr.*, 40, 900–913, <https://doi.org/10.1175/2009JPO4245.1>, 2010.

710 Takeshita, Y., Martz, T.R., Johnson, K.S., Plant, J.N., Gilbert, D., Riser, S.C., Neill, C., and Tilbrook, B.: A climatology-based quality control procedure for profiling float oxygen data, *J. Geophys. Res–Oceans.*, 118, 5640–5650, <https://doi.org/10.1002/jgrc.20399>, 2013.

715 Uchida, H., Kawano, T., Kaneko, I., and Fukasawa, M.: In situ calibration of optode-based oxygen sensors, *J. Atmos. Oceanic Technol.*, 25, 2271–2281, doi:10.1175/2008JTECHO549.1, 2008.

720 Van Der Boog, C. G., de Jong, M. F., Scheidat, M., Leopold, M. F., Geelhoed, S. C. V., Schulz, K., Dijkstra, H. A., Pietrzak, J. D., and Katsman, C. A.: Hydrographic and biological survey of a surface-intensified anticyclonic Eddy in the Caribbean Sea, *J. Geophys. Res–Oceans.*, 124, 6235–6251, <https://doi.org/10.1029/2018JC014877>, 2019.

Vukovich, F. M.: Changes in the Loop Current's Eddy shedding in the period 2001–2010, *International Journal of Oceanography*, 2012, 18, <https://doi.org/10.1155/2012/439042>, 2012.

725